BIOCHEMISTRY
including biophysical chemistry & molecular biology
Rapid Report

Biochemistry **2009,** *48,* 10483–10485 10483
DOI: 10.1021/bi901519q

IspG Enzyme Activity in the Deoxyxylulose Phosphate Pathway: Roles of the Iron−Sulfur Cluster†

Youli Xiao,‡ Georgia Zahariou,§ Yiannis Sanakis,§ and Pinghua Liu*,‡

‡*Department of Chemistry, Boston University, Boston, Massachusetts 02215, and* §*Institute of Materials Science, NCSR "Demokritos", 15310 Ag. Paraskevi, Attiki, Greece*

Received August 29, 2009; Revised Manuscript Received October 3, 2009

ABSTRACT: IspG is a [4Fe-4S] cluster-containing protein, and the $[4Fe\text{-}4S]^{+}$ species is proposed to be the catalytically relevant species. However, attempts reported in the literature failed to detect the $[4Fe\text{-}4S]^{+}$ species. In this study, using a potent reduction system, we have successfully detected the $[4Fe\text{-}4S]^{+}$ species with X-band EPR spectroscopy. In addition, we have improved the *Escherichia coli* IspG activity to 550 nmol min^{-1} mg^{-1}, which is ~20-fold greater than that of the NADPH−Fpr−FldA system in the literature.

Because of the commercial values of many isoprenoids, there is growing interest in producing them through bioengineering (*1*). An adequate supply of isoprenoid precursors, isopentenyl diphosphate (IPP, **9**) and its isomer dimethylallyl diphosphate [DMAPP, **10** (Scheme 1)], is one of the limiting factors for bioengineering-based isoprenoid production (*2*−*5*). Two pathways for the biosynthesis of IPP and DMAPP have been discovered: the deoxyxylulose phosphate (DXP) pathway in green algae, the chloroplasts of higher plants, and most eubacteria (*6*−*12*) and the mevalonic acid (MVA) pathway in animals, fungi, and Archaea (*13*).

Studies in bacteria and plants suggest that the carbon flow through the DXP pathway (Scheme 1) is regulated by a combination of three enzymes: the DXP synthase (DXS), the DXP reductoisomerase (DXR), and hydroxylmethylbutenyl diphosphate (HMBPP, **8**) reductase (IspH) (*1*). The enzymes catalyzing these earlier steps of the DXP pathway have been isolated with specific activities of 10−500 μmol min^{-1} mg^{-1} (*14*). Recently, we reported an in vitro *Escherichia coli* IspH activity of 30.4 μmol min^{-1} mg^{-1} (*6*). However, the highest reported in vitro *E. coli* IspG specific activity is 74−99 nmol min^{-1} mg^{-1}, which is almost 100-fold lower than those of the other DXP pathway enzymes (*7*, *8*). The inconsistency between the in vivo and in vitro studies suggests that a much greater specific activity for *E. coli* IspG is expected (*9*, *10*). In this paper, we improved the *E. coli* IspG activity by ~20-fold. In addition, using EPR spectroscopy, we demonstrated that the generation of an IspG $[4Fe\text{-}4S]^{+}$ species is the key reason for such a dramatic increase in activity.

IspG catalyzes the conversion of methylerythritol cyclic diphosphate (MEcPP, **7**) to (*E*)-4-hydroxy-3-methylbut-2-enyl diphosphate (HMBPP, **8**) (*7*, *15*−*17*). IspG is a [4Fe-4S] cluster-containing protein (*11*, *12*, *18*, *19*). Sequence analysis revealed that IspG has three conserved Cys residues, and a mutation of any of them leads to a decrease in activity of almost 10^5-fold (*7*). The IspG protein can be purified aerobically and then reconstituted in the presence of iron and sulfur to form its iron−sulfur cluster. The reconstituted IspG normally has four or five iron and sulfur atoms per IspG monomer. The *E. coli* IspG iron−sulfur cluster can also be assembled in vivo with the help from the *isc* operon, which is responsible for iron−sulfur cluster maturation. With the in vivo matured iron−sulfur cluster and purified anaerobically, IspG protein has a significantly greater activity relative to the IspG reconstituted in vitro (*7*).

Scheme 1: DXP Biosynthesis Pathway

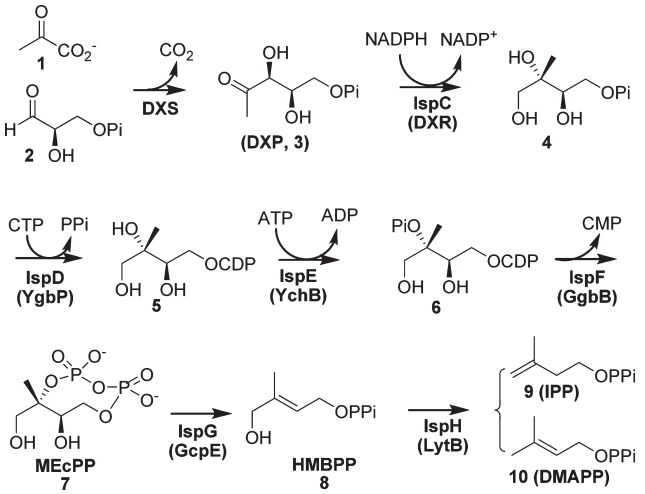

We coexpressed *E. coli* IspG with the *E. coli isc* operon and purified the strep-tagged IspG protein anaerobically to near homogeneity using streptavidin resin. The UV−visible absorption spectrum of the anaerobically purified IspG is consistent with the presence of iron−sulfur clusters, e.g., the features at ~320 and ~410 nm (Figure 1S of the Supporting Information). Under optimal conditions, the IspG protein with an A_{410}/A_{280} ratio of 0.32 was normally obtained without reconstitution (*7*, *11*). Using the methods reported by Fish (*20*) and Beinert (*21*), iron−sulfur analysis of the purified *E. coli* IspG indicated that there are 3.9 irons and 4.3 sulfurs per monomer, respectively.

Using chemically synthesized IspG substrate MEcPP (**8**) (*22*), purified IspG was assayed by ^{1}H NMR (Figures 2S and 3S of the Supporting Information) using the NADPH−Fpr−FldA system as the reducing system, which was proposed in the literature to be the in vivo IspG reducing system (*8*). Purified IspG has a specific activity of 15.6 nmol min^{-1} mg^{-1}, which is a few-fold lower than the best reported activity in the literature (*7*). This could be due to the fact that the ^{1}H NMR assay is an end point assay and tends to underestimate the activity.

†P.L. is supported by Boston University startup funds and NSF CAREER Award CHE-0748504.

*To whom correspondence should be addressed. Phone: (617) 353-2481. Fax: (617) 353-6466. E-mail: pinghua@bu.edu.

Published on Web 10/12/2009

In the literature, it was proposed that the $[4Fe\text{-}4S]^{2+/+}$ redox pair make up the catalytically relevant states (*11*, *12*, *18*, *19*, *23*). However, a $[4Fe\text{-}4S]^{+}$ cluster has not yet been convincingly detected. To study the roles of the IspG iron−sulfur cluster in catalysis, we characterized the anaerobically purified IspG protein at a concentration of 100 μM by X-band EPR spectroscopy.

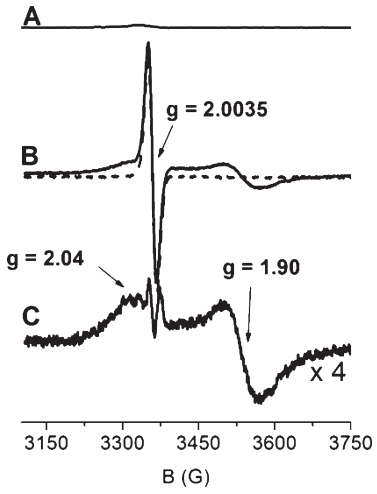

FIGURE 1: X-Band EPR spectra of *E. coli* IspG: (A) isolated IspG [100 μM IspG in 100 mM Tris-HCl buffer (pH 8.0)] and (B) IspG treated with a 10-fold excess of dithionite-reduced methyl viologen [100 μM IspG in 1.0 mM MV, 5.0 mM dithionite, and 100 mM Tris-HCl buffer (pH 8.0)]. The dashed line is the spectrum from a sample containing reduced methyl viologen only [1.0 mM MV, 5.0 mM dithionite, and 100 mM Tris-HCl buffer (pH 8.0)]. Under these experimental conditions, the signal from the reduced methyl viologen radical is saturated. Trace C is the difference of the two spectra in part B. A small radical $g = 2.0035$ signal on top of the $g = 2.04$ signal might be due to imperfect subtraction. EPR conditions: temperature, 12 K; microwave power, 2.2 mW; modulation amplitude, 5 G.

The as-isolated IspG is nearly EPR silent (Figure 1A), and the loss of the unique-iron site from the $[4Fe\text{-}4S]^{2+}$ cluster to form a $[3Fe\text{-}4S]^{+}$ cluster during IspG purification was not observed. Recent genetic studies suggest that the NADPH−Fpr−FldA system is the biologically relevant reduction system for *E. coli* IspG (*8*). However, similar to the results reported by Adedeji et al. for the *Thermus thermophilus* IspG studies, the reduction of *E. coli* IspG from a $[4Fe\text{-}4S]^{2+}$ state to a $[4Fe\text{-}4S]^{+}$ state was not observed when the NADPH−Fpr−FldA system was used as the reducing system (*7*, *24*). The lack of IspG iron−sulfur cluster reduction using the NADPH−Fpr−FldA system as the reducing system strongly suggests that an improvement in IspG activity might be achieved if a potent reduction system is used. Recently, we have demonstrated that this is the case for the IspH enzyme, which catalyzes the last step of the DXP pathway. With a potent reduction system, we improved the IspH activity by nearly 100-fold (*6*).

To test whether the same situation also holds true for the IspG enzyme, we assayed IspG using dithionite as a reductant in conjunction with alkylated bipyridinium salts as redox mediators (Table 1). The redox potentials of these alkylated bipyridinium salts range from −100 to −720 mV versus the normal hydrogen electrode (NHE) (Table 1) (*25*). When redox mediators with relatively high reduction potentials (greater than −300 mV) were used, there was low to no detectable IspG activity. Using redox mediators with reduction potentials of less than −300 mV, robust IspG activity was observed (Table 1).

The FldA FMN cofactor oxidized−semiquinone pair and semiquinone−hydroquinone pair reduction potentials are −245 and −455 mV, respectively (*31*). The Fpr FAD cofactor oxidized−semiquinone pair and the semiquinone−hydroquinone pair redox potentials are −308 and −268 mV, respectively (*32*). Results from our studies using redox mediators and the relatively

Table 1: Catalytic Activities from the *E. coli* IspG ^{1}H NMR Assay Using Redox Mediators with Different Reduction Potentials[a]

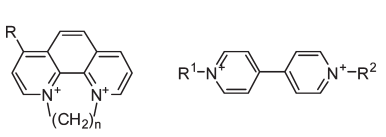

R = Cl, n = 3, **11a**
R = H, n = 3, **11b**
R = Me, n = 3, **11c**
R = H, n = 2, **11d**

$R^1 = R^2 = Me$, **12a** (MV)
$R^1 = Me$, $R^2 = H$, **12b**

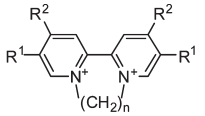

$R^1 = R^2 = H$, n = 2, **13a**
$R^1 = Me$, $R^2 = H$, n = 2, **13b**
$R^1 = H$, $R^2 = Me$, n = 2, **13c**
$R^1 = R^2 = H$, n = 3, **13d**
$R^1 = Me$, $R^2 = H$, n = 3, **13e**
$R^1 = H$, $R^2 = Me$, n = 3, **13f**

entry	mediator	conv.[b] (%)	activity[c] (nmol min^{-1} mg^{-1})	$E^{o\prime}$[d] (mV vs NHE)
1	**11a**	< 1	nd	−110 (*26*)
2	**11b**	< 1	nd	−130 (*27*)
3	**11c**	< 1	nd	−220 (*26*)
4	**11d**	< 1	nd	−250 (*27*)
5	**13a**	6.8	53.0	−312 (*28*)
6	**13b**	33	257	−442 (*28*)
7	**12a**	40	312	−446 (*29*)
8	**13c**	36	280	−450 (*28*)
9	**13d**	< 1	nd	−510 (*28*)
10	**13e**	17	132	−625 (*28*)
11	**13f**	21	163	−649 (*28*)
12	**12b**	21	163	−720 (*30*)
13	NADPH−Fpr−FldA[e]		15.6	

[a]The reaction was performed in 100 mM Tris-HCl (pH 8.0), 1.0 mM MEcPP, 1.0 μM IspG, 5.0 mM dithionite, and the appropriate mediator (10 mM) at 37 °C for 30 min. [b]The conversion was estimated based on the integration of signals from the methyl groups in HMBPP and MEcPP using 400 MHz ^{1}H NMR (see the Supporting Information). [c]Calculated from end point conversion. [d]Cited references. [e]The IspG concentration used in this assay was 5 μM.

high redox potentials of the Fpr FAD cofactor explain why the NADPH−FldA−Fpr system cannot reduce the IspG iron−sulfur cluster.

To provide further evidence to substantiate the conclusion given above, the formation of an IspG $[4Fe\text{-}4S]^{+}$ species was studied via X-band EPR spectroscopy (Figure 1B,C) using dithionite as the reductant and methyl viologen as the redox mediator because methyl viologen has a reduction potential of −446 mV (*29*). Reduced methyl viologen is a cation radical species (Figure 1B, dashed line) as characterized by the $g = 2.0035$ EPR signal ($\Delta H_{pp} = 16$ G), which is consistent with the data in the literature(*33*). After IspG was treated with a 10-fold molar excess of reduced methyl viologen, besides the signal from the excess reduced methyl viologen, new features developed (Figure 1B, solid line). Subtracting signals from reduced methyl viologen revealed a new axial signal (Figure 1C) comprising a $g \sim 2.04$ absorption peak and a $g \sim 1.90$ derivative feature. The temperature dependence and the saturation properties are consistent with that of a $[4Fe\text{-}4S]^{+}$ species. Spin quantitation of this species suggested that ∼0.3−0.4 spin per IspG monomer was formed when *E. coli* IspG was reduced by reduced methyl viologen. In contrast to previous studies, in which reduction of the IspG iron−sulfur cluster was difficult to achieve (*7*, *24*), the results from this work clearly indicate that the IspG iron−sulfur cluster can be reduced to the $[4Fe\text{-}4S]^{+}$ state if a potent reduction system is used.

Because the $[4Fe\text{-}4S]^{+}$ cluster is proposed to be a catalytically relevant species (*11*, *12*, *18*, *19*, *23*), with the successful detection of the $[4Fe\text{-}4S]^{+}$ state, we expected that significantly higher IspG activity should be achieved under our new assay condition. This hypothesis has been proven to be true. We measured IspG activity by monitoring the consumption of the reduced methyl viologen at 734 nm using its known extinction coefficients ($\varepsilon_{734} = 2665\ mM^{-1}\ cm^{-1}$, and $\varepsilon_{604} = 13600\ mM^{-1}\ cm^{-1}$) (*6*, *29*). The kinetic parameters for IspG-catalyzed conversion of MEcPP (**7**) to HMBPP (**8**) are as follows: $k_{cat} = 23.7\ min^{-1}$ ($550\ nmol\ min^{-1}\ mg^{-1}$), and $K_m = 311 \pm 21\ \mu M$ for **7** (Figure 5S of the Supporting Information). So far, this activity ($550\ nmol\ min^{-1}\ mg^{-1}$) is significantly greater than all previous reports on *E. coli* IspG studies (Table 2S of the Supporting Information). In our hands, the new IspG activity is more than 20-fold greater than that of the NADPH−FldA−Fpr system. The production of **8** under these assay conditions was also confirmed by ^{1}H NMR and high-resolution mass spectrometry after being isolated (Figure 6S of the Supporting Information). The identity of the product was supported by comparison with the spectroscopic properties of synthetic HMBPP (**8**) standard.

Recently, Adedeji et al. reported EPR characterization of IspG from a thermophile, *T. thermophilus* (*24*). When IspG from *T. thermophilus* was treated with dithionite, no signals corresponding to the $[4Fe\text{-}4S]^{+}$ cluster were detected, which suggests that dithionite alone does not reduce the IspG iron−sulfur cluster from a $[4Fe\text{-}4S]^{2+}$ state to a $[4Fe\text{-}4S]^{+}$ state. Interestingly, under steady-state conditions using dithionite as the reductant, rhombic EPR signals with g values of 2.087, 2.019, and 2.000 were detected. The authors suggested that the shape of the EPR signal is similar to that of a $[4Fe\text{-}4S]^{3+}$ species (*24*, *34*, *35*). Under steady-state conditions, the species can reach a level of 0.6 spin per IspG monomer. The authors also noticed that the behavior of this species does not match with that of the HiPiP $[4Fe\text{-}4S]^{3+}$ species reported in the literature (*24*).

Results from our studies clearly suggest that a redox mediator with a reduction potential of less than −300 mV is needed to achieve high IspG activity. Whether the $[4Fe\text{-}4S]^{3+}$ cluster suggested by Adedeji et al. for the *T. thermophilus* enzyme exists for *E. coli* IspG is still under investigation. In addition, the *E. coli* IspG activity from our studies is the best activity obtained so far, yet this activity is still at least 1 order of magnitude lower than those of the other enzymes of the DXP pathway. If indeed IspG is not the rate-limiting step in the DXP pathway, it may be that some other factors absent from our in vitro assay system are required to achieve maximal IspG activity. This issue is also currently under investigation.

SUPPORTING INFORMATION AVAILABLE

Additional references and results. This material is available free of charge via the Internet at http://pubs.acs.org.

REFERENCES

1. Rodríguez-Concepción, M. (2006) *Phytochem. Rev. 5*, 1–15.
2. Verpoorte, R., van der Heijden, R., ten Hoopen, H. J. G., and Memelink, J. (1999) *Biotechnol. Lett. 21*, 467–479.
3. Klein-Marcuschamer, D., Ajikumar, P. K., and Stephanopoulos, G. (2007) *Trends Biotechnol. 25*, 417–424.
4. Mahmoud, S. S., and Croteau, R. B. (2002) *Trends Plant Sci. 7*, 366–373.
5. Arsenault, P. R., Wobbe, K. K., and Weathers, P. J. (2008) *Curr. Med. Chem. 15*, 2886–2896.
6. Xiao, Y., Chu, L., Sanakis, Y., and Liu, P. (2009) *J. Am. Chem. Soc. 131*, 9931–9933.
7. Zepeck, F., Grawert, T., Kaiser, J., Schramek, N., Eisenreich, W., Bacher, A., and Rohdich, F. (2005) *J. Org. Chem. 70*, 9168–9174.
8. Puan, K. J., Wang, H., Dairi, T., Kuzuyama, T., and Morita, C. T. (2005) *FEBS Lett. 579*, 3802–3806.
9. Flores-Perez, U.; et al. (2008) *Biochem. Biophys. Res. Commun. 371*, 510–514.
10. Rivasseau, C.; et al. (2009) *Plant Cell Environ. 32*, 82–92.
11. Seemann, M.; et al. (2002) *Angew. Chem., Int. Ed. 41*, 4337–4339.
12. Rohdich, F.; et al. (2003) *Proc. Natl. Acad. Sci. U.S.A. 100*, 1586–1591.
13. Eisenreich, W., Bacher, A., Arigoni, D., and Rohdich, F. (2004) *Cell. Mol. Life Sci. 61*, 1401–1426.
14. Rohdich, F., Kis, K., Bacher, A., and Eisenreich, W. (2001) *Curr. Opin. Chem. Biol. 5*, 535–540.
15. Hecht, S.; et al. (2001) *Proc. Natl. Acad. Sci. U.S.A. 98*, 14837–14842.
16. Campos, N., Rodriguez-Concepcion, M., Seemann, M., Rohmer, M., and Boronat, A. (2001) *FEBS Lett. 488*, 170–173.
17. Kollas, A. K.; et al. (2002) *FEBS Lett. 532*, 432–436.
18. Seemann, M.; et al. (2005) *J. Biol. Inorg. Chem. 10*, 131–137.
19. Loiseau, L.; et al. (2007) *Proc. Natl. Acad. Sci. U.S.A. 104*, 13626–13631.
20. Fish, W. W. (1988) *Methods Enzymol. 158*, 357–364.
21. Beinert, H. (1983) *Anal. Biochem. 131*, 373–378.
22. Urbansky, M., Davis, C. E., Surjan, J. D., and Coates, R. M. (2004) *Org. Lett. 6*, 135–138.
23. Brandt, W., Dessoy, M. A., Fulhorst, M., Gao, W., Zenk, M. H., and Wessjohann, L. A. (2004) *ChemBioChem 5*, 311–323.
24. Adedeji, D., Hernandez, H., Wiesner, J., Kohler, U., Jomaa, H., and Duin, E. C. (2007) *FEBS Lett. 581*, 279–283.
25. Fultz, M. L., and Durst, R. A. (1982) *Anal. Chim. Acta 140*, 1–18.
26. Miller, D., and Mclendon, G. (1981) *Inorg. Chem. 20*, 950–953.
27. Tsukahara, K., and Wilkins, R. G. (1985) *J. Am. Chem. Soc. 107*, 2632–2635.
28. Alber, K. S., Hahn, T. K., Jones, M. L., Fountain, K. R., and Van Galen, D. A. (1995) *J. Electroanal. Chem. 383*, 119–126.
29. Mayhew, S. G. (1978) *Eur. J. Biochem. 85*, 535–547.
30. Guo, M., Sulc, F., Ribbe, M. W., Farmer, P. J., and Burgess, B. K. (2002) *J. Am. Chem. Soc. 124*, 12100–12101.
31. Vetter, H., and Knappe, J. (1971) *Hoppe-Seyler's Z. Physiol. Chem. 352*, 433–446.
32. McIver, L.; et al. (1998) *Eur. J. Biochem. 257*, 577–585.
33. Colaneri, M. J., Kevan, L., Thompson, D. H. P., and Hurst, J. K. (1987) *J. Phys. Chem. 91*, 4072–4077.
34. Antanaitis, B. C., and Moss, T. H. (1975) *Biochim. Biophys. Acta 405*, 262–279.
35. Dunham, W. R., Hagen, W. R., Fee, J. A., Sands, R. H., Dunbar, J. B., and Humblet, C. (1991) *Biochim. Biophys. Acta 1079*, 253–262.